Analysis and QSAR Modeling of Human Intestinal Transporter Database

T. J. Tkacik [1,2]

Advisor: Diane Pozefsky [1]

April 25, 2014

[1] Department of Computer Science, University of North Carolina at Chapel Hill

[2] Department of Chemistry, University of North Carolina at Chapel Hill

Abstract

Membrane transport proteins are the molecular gatekeepers that regulate the movement of chemicals into and out of every cell of every living organism.[1] In this study, a cheminformatics approach was taken to predict the substrate and inhibitory activities of 14 major human intestinal transporters using quantitative structure-activity relationship (QSAR) models built from 56 datasets. Dataset compounds were represented using CDK or Dragon descriptors and modeled using random forests (RF), support vector machines (SVM), and k-nearest neighbors (kNN). In all, 274 predictors passed all cut-offs. The predictive power of these predictors, as quantified by the external coefficient of determination (R^2) of regression predictors and correct classification rate (CCR) of classification predictors, was analyzed for correlations with characterizing data of the original datasets. Dataset size, represented by the logarithm of the cardinality; a modelability index (MODI), defined previously for binary datasets and extended to continuous datasets here; and the homology group of the represented transporter were each found to have statistically significant effects on predictive power. However, true validation of QSAR predictors requires additional laboratory experimentation.

Abbreviations

ABC	ATP-Binding Cassette superfamily of proteins	**MRP1-5**	Multidrug Resistance- associated Proteins 1-5
AD	Applicability Domain	**NBD**	Nucleotide-Binding Domain
ASBT	Apical Sodium-dependent Bile acid Transporter	**NTCP**	Sodium-Taurocholate Cotransporting Polypeptide
ATP	Adenosine TriPhosphate	**OATP2B1**	Organic Anion Transport Protein 2B 1
BCRP	Breast Cancer Resistance Protein	**OCT1**	Organic Cation Transporter 1
BSEP	Bile Salt export Pump	**PEPT1**	PEPtide Transporter 1
CAS	Chemical Abstract Services	**QSAR**	Quantitative Structure- Activity Relationship
CCR	Correct Classification Rate	**R2**	Coefficient of Determination
CDK	Chemistry Development Kit	**RF**	Random Forest
GA	Genetic Algorithm	**SA**	Simulated Annealing
IC50	Half maximal Inhibitory Concentration	**SDF**	Structure Data Format
kNN	k-Nearest Neighbor	**SLC**	SoLute Carrier family of proteins
MCT1	MonoCarboxylate Transporter 1	**SMILES**	Simplified Molecular Input Line Entry Specification
MDR1	MultiDrug Resistance Protein 1	**SVM**	Support Vector Machines
MODI	MODelability Index	**TMD**	TransMembrane Domain

Glossary of Terms

Amino Acids	the building blocks of proteins	**Homology**	the degree of conservation in amino acid sequences
Auto Scaling	normalization by standard deviation	***In silico***	conducted in simulation
Chemical Descriptors	quantified descriptions of the salient aspects of a compound	***In vitro***	conducted in laboratory setting
Cheminformatics	the application of information techniques to chemical data	***In vivo***	conducted in biological system
Chemistry space	the set of all energetically stable compounds	**Inhibitor**	a chemical that blocks a protein's active site
Chirality	asymmetry such that the molecule is different from its mirror image	**Pharmacophore**	abstract description of features of an active site
Combinatorial chemistry	chemical synthetic methods that produce entire compound libraries from a single process	**Range Scaling**	normalization by the range of values
Electrochemical potential	the combined effects of concentration and electrical potential	**Substrate**	a chemical that binds to a protein's active site
High-throughput screening	robotic or otherwise automated screening methods	**Transportome**	the set of all expressed genes corresponding to membrane transport

Background

Major Human Transporters

Drug resistance is mediated by nearly 600 identified human transport proteins, and it is assumed that at least 5% (>2000) of human genes are transport-related.[1-3] These transporters largely determine drug resistance by absorbing from and expelling chemicals into the intestines. Membrane transporters are the protein doorways responsible for facilitating and regulating the movement of both biological and pharmaceutical chemicals across the cell membrane.[1] Transporters may move chemicals into (importers) or out of (exporters) the cell and to or from the intestine (apical side) or bloodstream (basal side). Individual transporter-doorways, however, are unlocked by and translocate only a specific profile of chemical-keys called substrates. In addition, chemicals may act as inhibitors by preventing the transporter from moving substrates. Determining the factors that dictate how a drug interacts with major human transport proteins is a critical challenge for drug discovery.

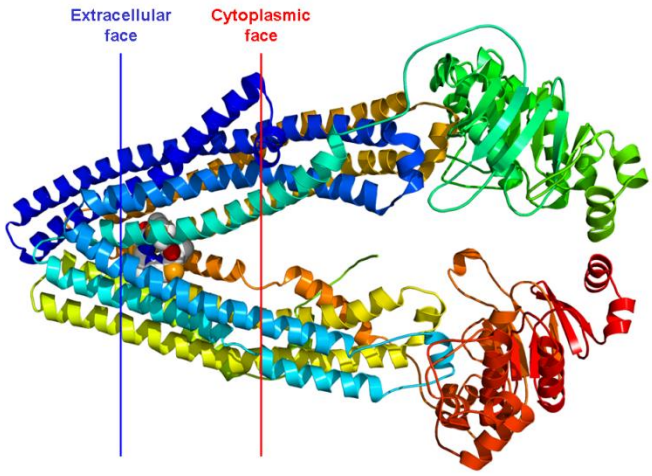

Figure 1. Crystallographic structure of mouse MDR3 protein illustrating the tremendous complexity of membrane transport proteins. The protein is rainbow colored from blue (C-terminus) to red (N-terminus). Approximate positioning of the extracellular (blue) and cytoplasmic (red) faces of the cell membrane is identified by the overlaid lines.[5]

The difficulty in predicting drug resistance, however, is compounded by the sheer complexity of the individual transporters. P-glycoprotein (MDR1) is the archetypal human ABC transporter, being the most medically relevant and well-studied. MDR1, Figure 1, is composed of 1280 amino acids (170 kDa) arranged as a single polypeptide.[2] Although the corresponding gene has been mapped, the crystal structure observed, and the amino acid sequence recorded, determining the actual mechanism of poly-specific substrate selection is still a major challenge for current bioinformatic techniques.[4] Alternative methods in the field of cheminformatics attempt to predict the interaction between substrate and protein without explicitly modelling the transporter active site or the mechanism of selection and transport.[6]

In this study, we look at members of two major transporter families: the ATP-binding cassette (ABC) superfamily and the solute carrier (SLC) group. Collectively, these groups include the majority of identified proteins that contribute to drug resistance and susceptibility, and understanding their biological differences may help explain differences in our ability to predict their behavior.

ATP-Binding Cassette (ABC) Superfamily

The ABC superfamily of transporters is fundamental to life as it evolved on Earth; members are believed to be present in every cell of every living organism.[2] All ABC transporters have two distinct substructures: a transmembrane domain (TMD, a portion of the protein that tunnels through the cell membrane) and cytosolic nucleotide binding domain (NBD). ABC proteins actively transport substrates through a series of conformational changes in the TMD that are initiated by the binding and hydrolysis of adenosine triphosphate (ATP, the cell's energy molecule) to the NBD. Although the NBD is very similar in all ABC transporters, the TMD vary widely, corresponding to variations in compatible substrates.

Solute Carrier (SLC) Group

In contrast to the evolutionary relatedness of ABC transporters, membership in the SLC group is functional, encompassing all families of transmembrane solute transporters that are not primary active transporters, ion channels, nor water channels. Accordingly, different SLC subfamilies exhibit little structural similarity, also referred to has homology.[3]

Mechanisms of Transport

Membrane transporters form doorways through the cell membrane and operate by one of three means:

- *Passive transporters* allow substrates to move naturally across the membrane from regions of high electrochemical potential to regions of low potential. This flow down an electrochemical gradient is energetically favorable and requires no additional energy.
- *Primary active transporters* are molecular motors that utilize an energy source, usually ATP hydrolysis, to drive the movement of substrate.
- *Secondary active transporters* are molecular turbines that couple the movement of two substrates simultaneously. The flow of one substrate down its gradient is used to power the movement of the other such that the overall energy change is still favorable.

ABC proteins undergo primary active transport while the SLC group includes both passive and secondary active transporters.

Cheminformatics

Although the intersection of chemistry and informatics had been established by the mid-1960s, the term "cheminformatics" was coined by F. K. Brown in 1998 as

> "the mixing of those information resources to transform data into information and information into knowledge for the intended purpose of making better decisions faster in the area of drug lead identification and optimization."[7,8]

One year later, at the August 1999 meeting of the American Chemical Society, G. Paris broadened to the term to

> "[encompass] the design, creation, organization, management, retrieval, analysis, dissemination, visualization, and use of chemical information."[6]

The new nomenclature was a symptom of the exploding interest in the field during the 1990s brought about both by advances in synthetic techniques and increases in computational power. In particular, the concurrent developments of combinatorial chemical synthesis and high-throughput screening allowed chemists to collect data hundreds of thousands times faster than before, the quantity of which conventional analytical techniques were simply unable to manage.[8-10]

In particular, cheminformatics seeks to reduce the time and capital costs of drug discovery by better identifying potential candidates earlier *in silico*. Current drug discovery techniques require an estimated fifteen-years and nearly two billion US dollars to bring a new drug into the market.[6,11] These costs are due to the immensity of the chemistry space as well as the rigor of clinical trials. Computational techniques, however, are relatively fast and cheap and can be employed to reduce the number of exploratory assays and studies necessary.[12-14]

Molecular Representation

Molecules are complex real-world objects. Even 3-dimensional topography models are little more than illustrative simplifications of what are in reality infinite fields of electron density associating infinitesimal points of mass and charge. Although many standards exist in practice, the task of representing molecules *in silico* is neither trivial nor complete. A database of molecules may be queried using the accepted common name or a unique registry number assigned by the Chemical Abstracts Services (CAS). More informative representations reference the chemical structure explicitly: the International Union of Pure and Applied Chemistry

Figure 2. Standard cheminformatic representations for aspirin.[6]

Name	Representation
Common Name	Aspirin
Synonyms	Acetylsalicylic acid, Ecotrin, Acenterine, Acylpyrin, Polopyryna, Acetophen, Acetosal, Aspergum
Empirical Formula	$C_9H_8O_4$
2D Structure	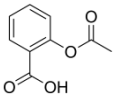
IUPAC Name	2-Acetoxybenzoic acid
CAS Registry Number	50-78-2
SMILES	CC(=O)OC1=CC=CC=C1C(=O)O
InChI	1S/C9H8O4/c1-6(10)13-8-5-3-2-4-7(8)9(11)12/h2-5H,1H3,(H,11,12)
Connection Table (SDF)	Aspirin *Comment Line* 21 21 0 0 0 0 0 0 0 999 V2000 6.3301 -0.5600 0.0000 C 0 0 0 0 0 0 0 0 0 0 0 0 4.5981 -1.5600 0.0000 C 0 0 0 0 0 0 0 0 0 0 0 0 6.3301 -1.5600 0.0000 C 0 0 0 0 0 0 0 0 0 0 0 0 5.4641 -2.0600 0.0000 C 0 0 0 0 0 0 0 0 0 0 0 0 2.0000 -0.0600 0.0000 C 0 0 0 0 0 0 0 0 0 0 0 0 5.4641 -0.0600 0.0000 C 0 0 0 0 0 0 0 0 0 0 0 0 4.5981 -0.5600 0.0000 C 0 0 0 0 0 0 0 0 0 0 0 0 4.5981 1.4400 0.0000 O 0 0 0 0 0 0 0 0 0 0 0 0 2.8660 -1.5600 0.0000 O 0 0 0 0 0 0 0 0 0 0 0 0 6.3301 1.4400 0.0000 O 0 0 0 0 0 0 0 0 0 0 0 0 5.4641 0.9400 0.0000 C 0 0 0 0 0 0 0 0 0 0 0 0 2.8660 -0.5600 0.0000 C 0 0 0 0 0 0 0 0 0 0 0 0 3.7321 -0.0600 0.0000 O 0 0 0 0 0 0 0 0 0 0 0 0 6.3301 2.0600 0.0000 H 0 0 0 0 0 0 0 0 0 0 0 0 6.8671 -0.2500 0.0000 H 0 0 0 0 0 0 0 0 0 0 0 0 4.0611 -1.8700 0.0000 H 0 0 0 0 0 0 0 0 0 0 0 0 6.8671 -1.8700 0.0000 H 0 0 0 0 0 0 0 0 0 0 0 0 5.4641 -2.6800 0.0000 H 0 0 0 0 0 0 0 0 0 0 0 0 2.3100 0.4769 0.0000 H 0 0 0 0 0 0 0 0 0 0 0 0 1.4631 0.2500 0.0000 H 0 0 0 0 0 0 0 0 0 0 0 0 1.6900 -0.5969 0.0000 H 0 0 0 0 0 0 0 0 0 0 0 0 6 7 2 0 0 0 0 1 6 1 0 0 0 0 6 11 1 0 0 0 0 2 7 1 0 0 0 0 7 13 1 0 0 0 0 1 3 2 0 0 0 0 10 11 1 0 0 0 0 8 11 2 0 0 0 0 2 4 2 0 0 0 0 12 13 1 0 0 0 0 5 12 1 0 0 0 0 9 12 2 0 0 0 0 3 4 1 0 0 0 0 1 15 1 0 0 0 0 2 16 1 0 0 0 0 3 17 1 0 0 0 0 10 14 1 0 0 0 0 4 18 1 0 0 0 0 5 19 1 0 0 0 0 5 20 1 0 0 0 0 5 21 1 0 0 0 0 M END $$$$

(IUPAC) has defined explicit nomenclature standards, Simplified Molecular Input Line Entry Specification (SMILES) defines rules for describing molecular structure using an ASCII string, and the Structure Data Format (SDF) standards are the most commonly used graph-based representation.[6] Figure 2 illustrates several standard representations for aspirin.

The structure itself is usually not useful for analysis, so descriptors are generated from the structural representation. Molecular descriptors are quantified features that describe the salient aspects of the compound. Both open-source, e.g. CDK, and privately licensed, e.g. Dragon, descriptor generators exist with their own individual sets of descriptors.[6] There are two primary classes of descriptors. Information-based descriptors encapsulate the structure of the compound and include descriptors for the molecular weight, the number of rotatable bonds, and Kier shape indices. Knowledge-based descriptors are calculated using known models and include estimates of the polarity in different regions of the compound. The Dragon descriptor set is much larger than CDK (2489 v. 202) and includes many more esoteric and hyper-specific descriptors, e.g. the frequency of carbon-fluorine atom pairs exactly 10 bonds apart. In general, there is a trade-off between interpretability and predictive usefulness.[13]

QSAR Modeling

Quantitative structure-activity relationship (QSAR) modelling may be described as the use of computational, analytical, and statistical methods to accurately and reliably predict or explain the properties or activities of chemical compounds provided only their structure.[15] Chemical activity can be defined as any quantifiable and observable behavior. It may be a classification (e.g. substrate or not), a regression (e.g. the rate of transport through a membrane), or a categorization into an ordered set of classes (e.g. highly active, active, or inactive).[16]

As early as 1869, Alexander Crum Brown and Thomas Richard Fraser proposed that a molecule's activity can be defined as a mathematical function of its structure.[6] Furthermore, the structure-activity relationship hypothesis states that similar compounds possess similar properties. Unfortunately, chemical similarity and diversity are oftentimes extremely difficult to define, and different measures of similarity may be relevant when considering different activities. QSAR modeling attempts to quantify a structure-activity relationship such that it may be used to identify priority compounds for experimental validation.

The predictive QSAR modeling workflow presented in Figure 3 has been adapted from Tropsha 2010.[15] The input to the QSAR workflow is always a dataset of compounds with experimentally confirmed chemical activities. Thus the quality of a QSAR predictor is fundamentally reliant on the quality of the experimental values and an accurate understanding and representation of the chemical structures. It is critical to curate the chemical dataset to ensure accurate structures and to remove any compounds that may not be informative to the model. If chirality-sensitive descriptors are not employed, all pairs of mirror images will be represented as duplicates; one must be removed, and any variance in their activities must be reconciled. In addition, any compounds should be removed that cannot be handled by current techniques, including organometallic complexes, inorganic compounds, salts, and mixtures.[15]

Any number of supervised learning techniques may then applied to the curated dataset to construct the predictor, but the workflow remains the same.[15] Firstly the dataset must be divided

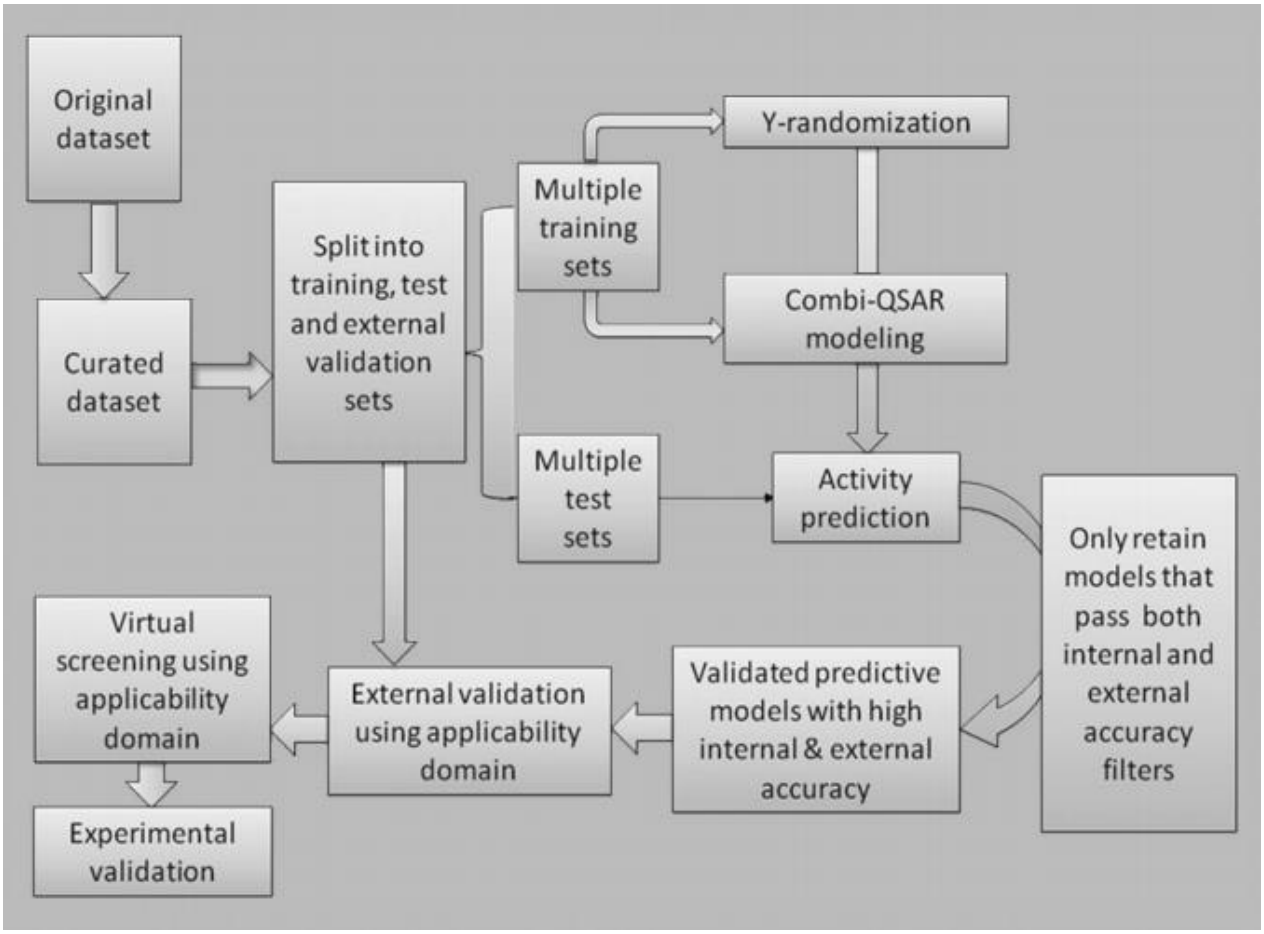

Figure 3. Predictive QSAR modeling workflow. [15]

into modeling and external sets. Usually many models are constructed from the modelling set, and the best models, as identified by some internal evaluation, are consolidated to form the predictor. To avoid overfitting, training is conducted using only the modelling set, and the external set is used to validate the predictor.[17] By considering the distribution of compounds, an applicability domain (AD) is applied to each model as well as the overall predictor that defines the subspace of the chemistry space for which the model has been validated.

Although there is a precedent for regulation based solely on predictive modelling,[18] a predictor should ideally be subject to laboratory validation. *In silico* high-throughput screening of the predictor on compound databases will identify additional compounds with activities of interest. The activities of some of these compounds should be determined experimentally to further validate the predictor.[15]

Modeling Major Human Transporters

The human transportome consists of the subset of the proteome devoted to membrane transporters. Recently, there have been several large-scale efforts to collect and organize the ever increasing amount of transportome data available.[19-23] Yet, until very recently, there has been little effort to model this substrate data with the corresponding explicit molecular structures.[1] In this study, 56 datasets comprised of 10,407 activity values corresponding to the interaction between 3,906 unique chemical compounds and 14 transporters were curated, characterized, and modeled using multiple QSAR algorithms. The quality of the QSAR predictors was analyzed to elucidate correlations with the chemical, biological, and numerical characters of the datasets.

Materials and Methods

Dataset Creation and Curation

Chemical-transporter interaction data were collected and curated by the Molecular Modeling Lab in the Eshelman School of Pharmacy at the University of North Carolina at Chapel Hill. Data were extracted from multiple publically available sources and consolidated into 56 datasets.[19-23] Equivalent records were compared and reconciled to form a single, harmonious database. Classification datasets were constructed by combining reports of substrate or inhibitory activity. Accordant reports were assigned values of 0 or 1, and ambiguous chemicals were not included. Inhibitor classification is defined at a specified threshold concentration for each dataset. Binding affinities are included as the negative log of either the

Michaelis-Menten constant of transportation (pK_m, the relative concentration of substrate needed to transport at a rate half of the maximum) or of the half maximal inhibitory concentration (pIC50, the relative concentration of inhibitor needed to reduce the rate of transport by half). In addition, datasets of pIC50 values are included for both general and specific hot ligands (the substrate whose transport is being inhibited).

Chemical structures were standardized by the Molecular Modeling Lab using PipelinePilot ver.6.15 (Accelrys) and the Standardizer module (ChemAxon).[1] Organometallic and poorly defined compounds were excluded from the database. In addition, polymers, identified as extreme molecular weight outliers, were also excluded. Remaining compounds were standardized and translated into their predominant and neutral form. The final curated database is available on Chembench.[26] The full, detailed process for data collection and curation has been previously described by Sedykh *et al.*[1]

Dataset Characterization

The 56 datasets were preliminarily characterized by their relevant transporter and by the parameters of the activity reported (see Tables 6 and 7 of the appendix). A summary of the number of compounds in the datasets is available in Table 1. Twenty-five datasets comprised of continuous values, and 31 contained binary assignments. Eighteen datasets reported substrate activity, and 38 reported inhibitory activity (see Figure 5).

Table 1. Summary of dataset cardinality.

Activity Type	Max	Min	Mean	St. Dev.
Classification (N = 31)	1585	34	228.3	313.7
Continuous (N = 25)	476	27	133.2	121.5

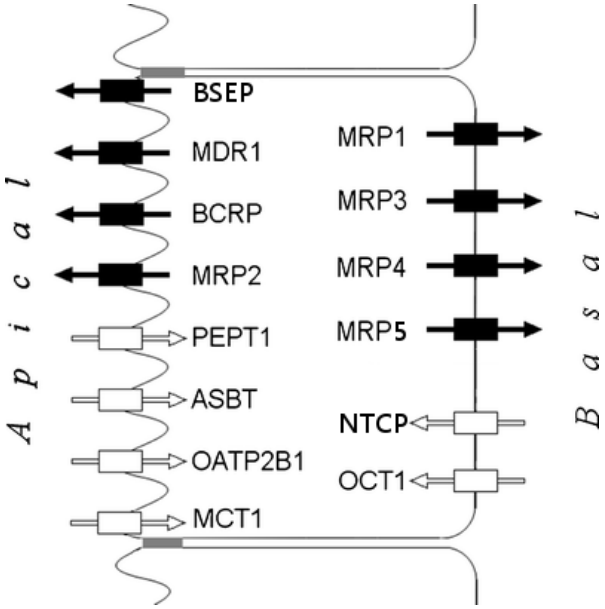

Transporters were also characterized by the physiological role in the human body (see Table 8 of the appendix and Figure 4).[24] In all, 14 transporters from the ABC and SLC groups are represented. Their membrane location, direction of flow, subfamily, and archetypal substrate are also reported and were included in the statistical analysis.

Figure 4. Localization of major intestinal transporters on intestinal skin cells. Rectangles with arrows represent transporters. ABC (black) and SLC (white) families are designated by color.[1]

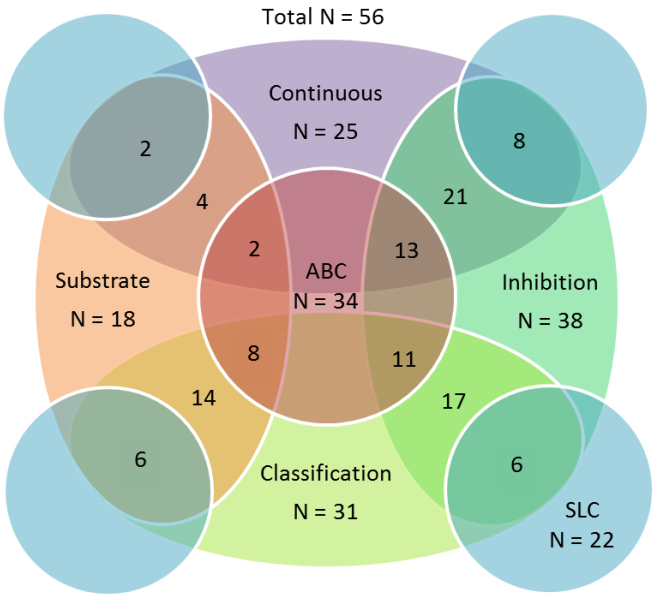

Figure 5. Distribution of the characterizations of datasets in the database. Note the bias towards inhibition datasets, especially among continuous datasets.

Descriptor Generation

Descriptors were generated for each dataset using both the open-source Chemistry Development Kit (CDK) ver.1.3 (202 descriptors) as well as Dragon ver.1.4.4 (Talete) with explicit hydrogens (2489 descriptors). Any descriptors that generated an error for at least one compound were dropped from the datasets. Descriptors were considered non-informative and dropped from individual datasets if they correlated completely with another descriptor or if they did not vary across compounds in that dataset. Counts of retained descriptors for individual classification and continuous datasets are listed in Tables 6 and 7 of the appendix and are summarized in Table 2.

Table 2. Summary of descriptors retained.

Descriptor Set	Max	Min	Mean	St. Dev.
CDK	162	127	151.6	8.4
Dragon	1420	835	1098.3	135.9

Modelability Index Calculation

In a recent publication, Golbraikh *et al.* proposed the use of a MODelability Index (MODI) to assess the goodness of a dataset for successful model building based on the frequency of activity cliffs (regions in the descriptor space where chemical activity changes rapidly).[25] They offer a definition for classification datasets computed from the number of dissimilar nearest neighbors present for each class in the dataset:

$$\mathrm{MODI}_{\mathrm{classification}} = \frac{1}{K}\sum_{i}^{K}\frac{N_i^{same}}{N_i^{total}} \quad (1)$$

where K is the number of classes, N_i^{same} is the number of compounds belonging to the ith class whose nearest neighbor belongs to the same class, and N_i^{total} is the total number of compounds in the ith class. Nearest neighbors are determined as the neighbor with the least Euclidean distance

from the compound in the entire descriptor space.[25] Because descriptors are generated from the chemical structure, the nearest neighbor will be the most structurally similar compound.

I offer a similar definition of MODI for continuous datasets for use and evaluation in this study:

$$\mathrm{MODI}_{\mathrm{regression}} = \frac{1}{N}\sum_{i}^{N}|z(a_i) - z(a_i')| \quad (2)$$

where N is the total number of compounds, $z(a_i)$ is the normalized activity of the ith compound, and $z(a_i')$ is the normalized activity of the neighbor nearest to the ith compound. Therefore MODI is calculated as the average number of standard deviations in activity between nearest neighbors.

MODI values were computed for each transporter dataset using Python ver.2.7.6 including the packages NumPy and scikit-learn ver.0.14. Descriptors were auto scaled before calculating neighbor distances. MODI values for individual classification and continuous datasets are listed in Tables 6 and 7 of the appendix and are summarized in Table 3.

Table 3. Summary of dataset modelability indices.

Activity Type	Max	Min	Mean	St. Dev.
Classification (N = 31)	0.98	0.39	0.75	0.11
Continuous (N = 25)	0.58	0.06	0.31	0.13

QSAR Modeling

Quantitative structure-activity relationship (QSAR) predictors were created using the Carolina Cheminformatics Workbench (Chembench) developed by the Carolina Exploratory Center for Cheminformatics Research (CECCR) and according to the workflow outlined in Figure 3.[26] Random forests (RFs) were generated using the randomForest package for R ver.4.6-7, support vector machines (SVMs) were constructed using an grid-search built on libsvm, and k-nearest neighbors (kNN) predictors were prepared using an internally developed KNN+ ver.2.82. Meta-parameters for each predictor type were controlled across datasets.

Datasets were split into five equal folds for external cross-validation. Separate predictors were generated and evaluated for each external fold and then consolidated into a single consensus predictor. Internal test sets were selected by sphere exclusion for datasets with fewer than 300 compounds and randomly otherwise. Predictors were created for each dataset using either CDK or Dragon descriptor sets.

Continuous datasets were modeled using RF, SVM, and kNN. The kNN predictors were trained using a genetic algorithm (GA-kNN) for datasets with greater than 150 compounds and both GA-kNN and simulated annealing (SA-kNN) otherwise. Descriptors were normalized using range scaling. Predictors were evaluated by the average coefficient of determination (R^2) of the five folds:

$$R^2 = \frac{\mathrm{SSR}}{\mathrm{SST}} = 1 - \frac{\mathrm{SSE}}{\mathrm{SST}} = 1 - \frac{\sum_i (y_i - \hat{y}_i)^2}{\sum_i (y_i - \bar{y})^2} \quad (3)$$

where y_i is the observed activity of the ith compound, $\hat{y}_i$ is the predicted activity of the ith compound, and $\bar{y}$ is the average activity of all compounds.[15] Note that because the model predictions are not a linear best fit, the sum of squared errors (SSE) may be greater than the total sum of squares (SST) in the observed activities. Therefore R^2 values may be negative.[17] Coefficients of determination for individual regression predictors, reported as the mean of five cross-validation folds, are shown in Table 9 of the appendix and are summarized in Table 4.

Table 4. Summary of coefficients of determination for regression predictors.

	Max	Min	Mean	St. Dev.
R^2	0.82	-0.20	0.37	0.22

As will be shown, modeling technique was not found to have a significant effect on predictive power. Therefore, because of its rapid modeling time, classification datasets were modeled using RF only. Four predictors were generated for each dataset corresponding to each combination of range or auto scaled CDK or Dragon descriptors. Predictors were evaluated by the overall correct classification rate (CCR) of the five folds:

$$\mathrm{CCR} = \frac{1}{K} \sum_i^K \frac{N_i^{correct}}{N_i^{total}} \quad (4)$$

where K is the number of classes (K = 2 for binary datasets), $N_{i,correct}$ is the number of correctly classified compounds in the ith class, and $N_{i,total}$ is the total number of compounds in the ith class. Previous studies have identified a CCR of 0.7 to be the threshold for acceptable predictive power.[15,25] CCR, reported as the mean of five cross-validation folds, are shown in Table 10 of the appendix and are summarized in Table 5.

Table 5. Summary of correct classification rates for classification predictors.

	Max	Min	Mean	St. Dev.
CCR	0.96	0.48	0.79	0.09

Model Fortification

Predictors were subjected to several additional thresholds throughout the modeling process to maximize predictive power. Datasets with fewer than 30 compounds were not modeled (N = 2). Individual models were required to present a squared leave-one-out cross-validation correlation coefficient (Q^2) of at least 0.6 to be accepted.

In addition, stochastic models were identified using y-randomization. This process randomly redistributes activities to the compounds in the modeling set, constructs a predictor, and calculates a CCR or R^2 using a fraction of the modeling set as an evaluation set. Five y-randomized predictors are constructed in this way such that a one-tailed *t*-test could be conducted to determine the probability of obtaining the CCR or R^2 of the true-activity predictor with randomized values. If the p-value was greater than 0.05, the models built using the real data were deemed unreliable and rejected.

An applicability domain (AD) of 0.5 standard deviations was also applied to each model of kNN predictors. The standard deviation in Euclidean distance in the descriptor space between each compound and its k nearest neighbors was calculated. Models were ignored during prediction and evaluation if the new compound did not have at least k neighbors within 0.5 standard deviations.

In all, 274 predictors passed all cut-offs. The five datasets with fewer than 50 compounds (N = 5) failed to produce any kNN models that passed all cut-offs. In addition, two datasets with 51 compounds failed to generate adequate models for a single kNN predictor each.

Statistical Analysis

Dataset characterization data and predictor quality data were prepared for analysis using Excel ver.14.0 (Microsoft). Statistical analyses were conducted using Stata ver.13.0 (StataCorp).

Results and Discussion

A series of linear regression analyses were conducted to reveal correlations between the biological, chemical, and numerical characteristics of the datasets and the modelability as expressed by the coefficient of determination (R^2) or correct classification rate (CCR) of the predictor. These results may be used to improve future QSAR studies as well as to identify relevant properties of the transporter pharmacophores that have not previously been described.

Quantifying Predictive Power

The coefficient of determination (R^2) calculated for continuous predictors is a measure of the sum of squares of the external validation. Unfortunately, this value does not lend itself well to linear regression. In addition, some values of R^2 were found to be negative. Therefore a transformed root of squares (R^1) was used for analysis:

$$R^1 = 1 - \sqrt{1 - R^2} \tag{5}$$

where R^2 is the coefficient of determination.

Although it may be tempting to make conclusions about the relative success of regression and classification QSAR predictors, it should be emphasized that R^1 (equations (3) and (5)) and CCR (equation (4)) are distinct evaluation measures that are not comparable. Both R^1 and CCR asymptotically approach 1.0 as external prediction improves. However, while R^1 ranges to negative infinity, CCR has a minimal value of zero. A random assignment of regression predictions from the observed distribution will result in an R of 0.0, but a random classification will result in a CCR of the inverse of the number of classes (CCR = 0.5 for binary data sets). Therefore all analyses were conducted separately on either regression or classification predictors.

Numerical Characteristics

Not surprisingly, the size of a dataset was found to have a significant positive correlation ($p < 0.001$) with predictive power for both regression and classification datasets. Furthermore, this correlation is best realized when the dataset size is represented by the logarithm of the cardinality. Figures 6 and 7 plot the R^1 values for each regression predictor and CCRs for each classification predictor, respectively, against the size of the original dataset.

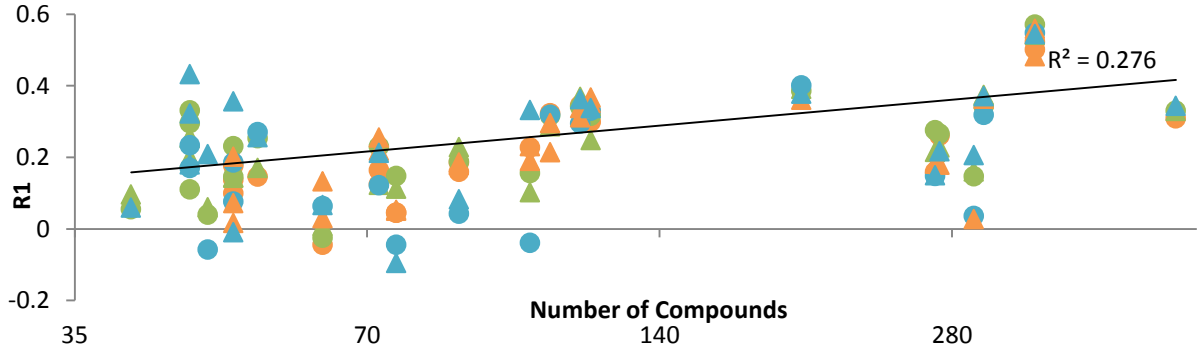

Figure 6. Correlations between the logarithm of the number of compounds and the R^1 of regression predictors. CDK (circles) and Dragon (triangles) descriptors are denoted by shape. RF (green), SVM (blue) and kNN (orange) are denoted by color.

In addition, QSAR modeling technique, descriptor type, and descriptor scaling are denoted for each datum in Figures 6 and 7. None of these characteristics, nor the number of descriptors, had a statistically significant effect on predictive power for either continuous or classification datasets when controlling for the size of the dataset.

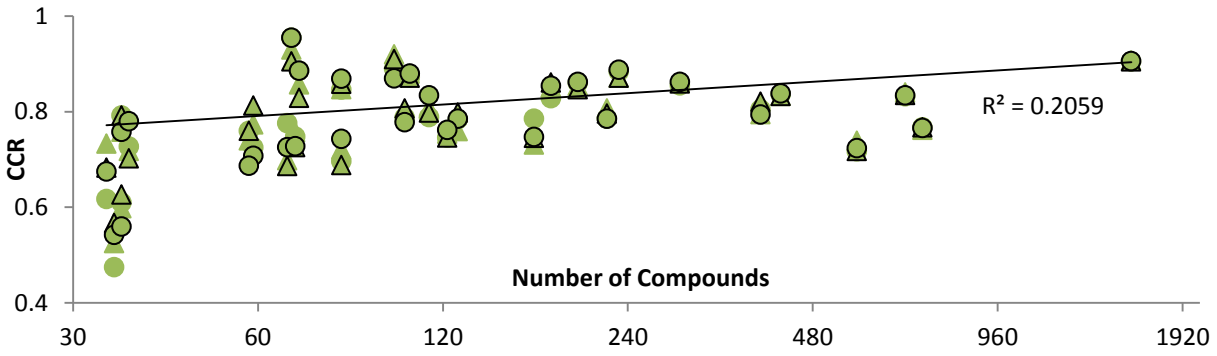

Figure 7. Correlations between the logarithm of the number of compounds and the CCR of classification predictors. CDK (circles) and Dragon (triangles) descriptors are denoted by shape. Auto scaling is indicated by the presence of a black border.

Modelability Indices

Classification MODI

The definition of a Modelability Index (MODI) offered by Golbraikh *et al.*[25] and presented again here as equation (1) was found to be a strong indicator of the predictive power of RF classification transporter datasets. A significant correlation (R^2 = 0.72) was found between MODI and a predictor's external CCR. Figure 8 is a plot of each predictor's CCR against the MODI of its original dataset. Using the threshold for modelability also offered by Golbraikh *et al.* (CCR > 0.7), MODI can be used to reliably estimate whether a dataset may yield an acceptable predictor. Nearly all (N = 107 of 112) predictors built from datasets with MODI above 0.64 resulted in a CCR greater than 0.7.

In addition, descriptor type, and by extension the number of descriptors, was not found to affect the MODI of a dataset. Figure 8 is a plot of the MODI calculated using Dragon descriptors versus the MODI calculated using CDK descriptors for each classification dataset. A significant correlation (R^2 = 0.77) was determined for a linear regression through the origin. Note that only two datasets deviate from this trend: datasets 41 and 40 located in the lower left of Figure 9. The discrepancy in MODI implies that the compounds in these datasets are represented differently in some significant way in the different descriptor spaces. These datasets are both concerned with

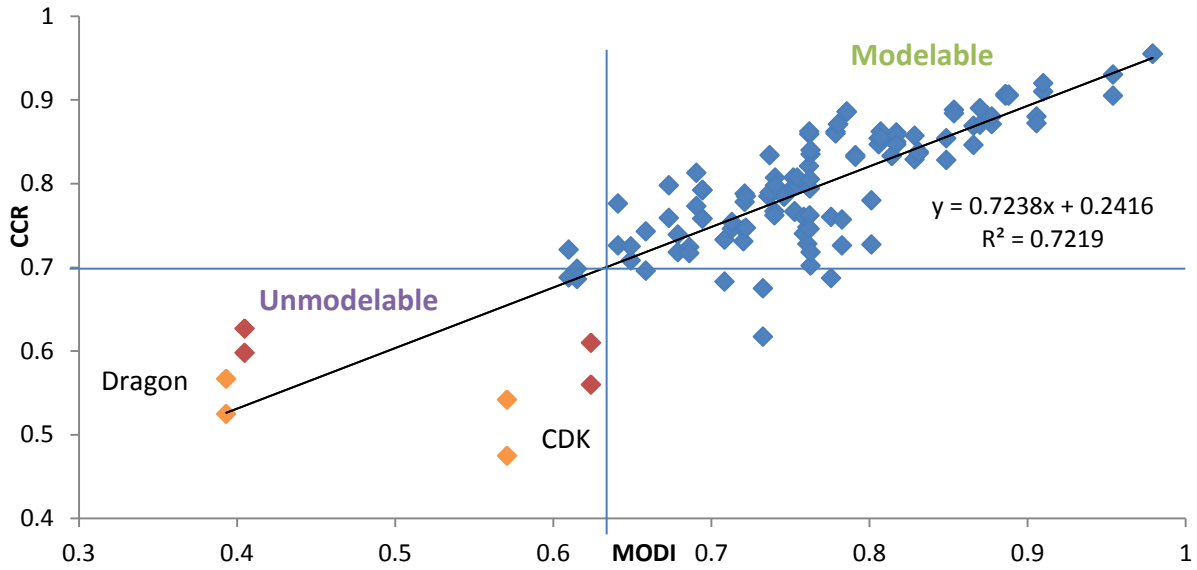

Figure 8. Correlation between the CCR of classification predictors and the MODI of their original datasets. The threshold for modelability is marked at CCR = 0.7 and correspondingly at MODI = 0.63. Datasets 40 (red) and 41(orange) are identified from Figure 9.

the inhibition of MRP3 at different thresholds. Cross referencing Figure 8 reveals that the MODI calculated using Dragon descriptors better predicted the CCR of the resultant predictors. Therefore it may be inferred that CDK does not include some key descriptors relevant to MRP3 inhibition. However, any major conclusions from these datasets should be avoided because they contain relatively few compounds (N = 36 and 35).

In addition, this set of datasets is biased toward modelable datasets. Additional predictors with CCR between 0.5 and 0.7 would need to be studied to verify the correlation in the unmodelable quadrant of Figure 8.

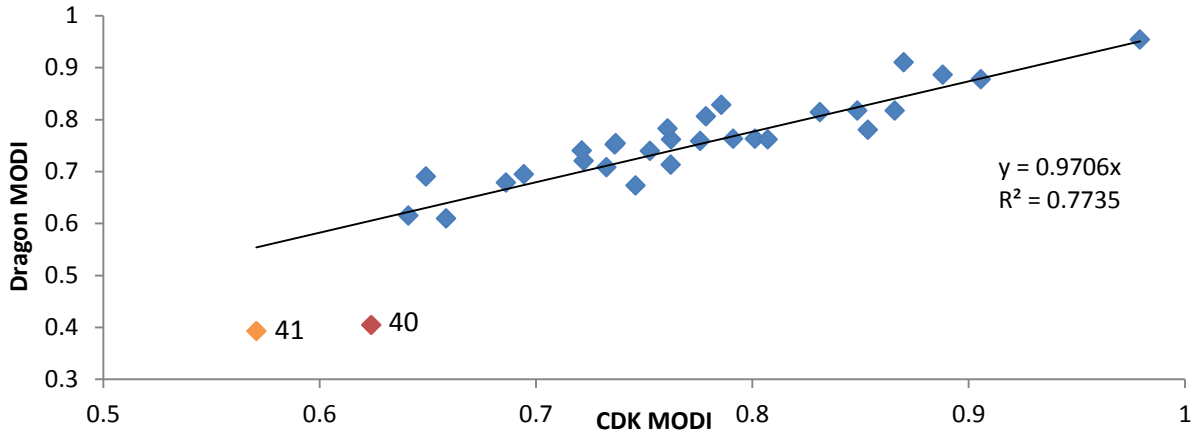

Figure 9. Correlation between MODI calculated using Dragon descriptors and CDK descriptors for each classification dataset. Datasets 40 (red) and 41(orange) are identified as significant outliers.

Continuous MODI

A novel definition for the MODI of continuous datasets was introduced in equation (2). A significant correlation (R^2 = 0.59) was found between values calculated using this definition of MODI and a regression predictor's R^1 value. Figure 10 illustrates this relationship with descriptor type and modeling technique identified. Using a coefficient of determination of R^2 > 0.5 as the threshold for modelability[15] corresponds to a root of squares of roughly R^1 > 0.3. Therefore I propose a heuristic threshold of MODI > 0.35 to estimate the modelability of continuous datasets. This cutoff deviates from the regression line to increase sensitivity without sacrificing precision in this set.

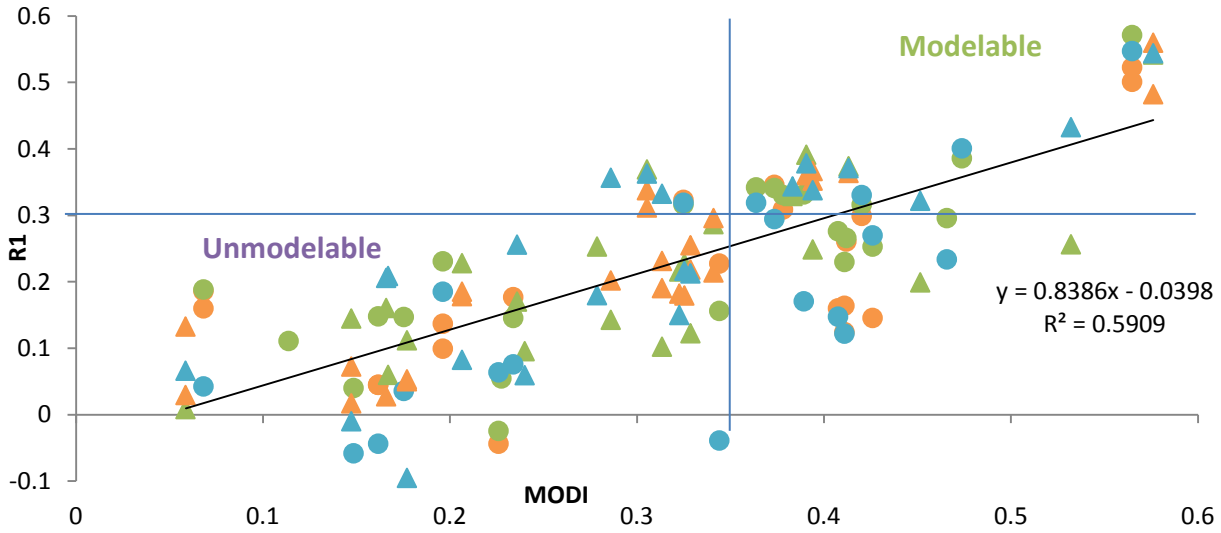

Figure 10. Correlation between the R^1 of regression predictors and the MODI of their original datasets. The threshold for modelability is marked at R^1 = 0.3, and a corresponding cutoff is proposed at MODI = 0.35. CDK (circles) and Dragon (triangles) descriptors are denoted by shape. RF (green), SVM (blue) and kNN (orange) are denoted by color.

Biological Characteristics

The membrane transporters were divided into homologous groups for additional analysis. Because all ABC transporters are related, this process grouped ABC together and SLC transporters into subfamilies. A statistically significant correlation was determined between this grouping and the predictive power of classification datasets. In particular, predictors concerning SLC transporters reported CCRs 0.089 greater (p < 0.001) than ABC predictors, on average. This correlation persists when dataset size and MODI are included in the regression. Figure 11 illustrates the way that ABC predictors evaluated more poorly, even when the original datasets computed similar MODI. This indicates that there are additional factors affecting modelability

besides those captured by MODI. This trend may result from the interaction with ATP as the energy source or it may indicate that ABC transporters are reliant on the selectivity of multiple external binding proteins.

Additional features characterizing the membrane transporter and activity measure were analyzed as well. The location of the transporter *in vivo*, whether in the basal or apical membranes, was not found to be significant for predictive power. Whether the dataset included inhibitor or substrate activity data, however, was significant for both classification and regression predictors when controlling for dataset size. Curiously, classification inhibitor datasets predicted CCR 0.034 less (p = 0.022) than their substrate counterparts on average, but continuous inhibitor datasets evaluated with R^1 0.080 greater (p = 0.007) on average. This discrepancy is not quickly explained, and additional research is needed to determine which, if either, correlation is accurate.

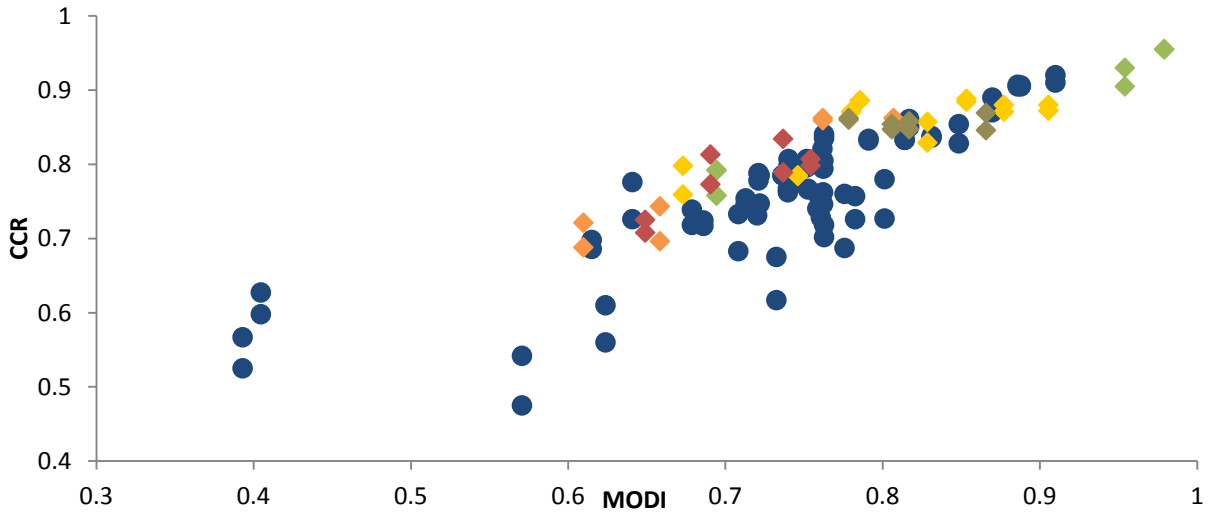

Figure 11. CCR of predictors by homology group: ABC (blue), SLC10 (yellow), SLC15 (orange), SLC16 (green), SLC22 (brown), and SLCO (red).

Conclusions

Membrane transport proteins are directly responsible for the movement of chemicals into and out of each cell, so predicting their interaction with potential drug candidates is an important challenge for drug discovery.[1] Quantitative structure-activity relationship (QSAR) modeling, as part of the greater field of cheminformatics, attempts to predict the activity of new compounds by comparing their structures with the structures of compounds with known interactions. This technique was applied to 56 datasets concerning 14 major human transporters. A modelability index (MODI) for chemical datasets of continuous activities was developed to mimic an existing

MODI for classification datasets as a heuristic device for estimating predictive power. Dataset cardinality and MODI were found to have significant effects on predictive power, but modeling technique and descriptor type were not. In addition, transporter homology group was found to have a significant effect such that ABC datasets modeled more poorly, on average. This suggests that the mechanism of substrate selection of ABC proteins is more complex than that of SLC proteins. True validation of QSAR predictors requires laboratory experimentation, which was not available for this study.[15] Therefore additional research is needed to confirm the predictive powers of each dataset and verify the correlations observed.

Acknowledgements

I would like to express my deepest thanks to Professor Pozefsky for her guidance and support throughout the course of this study in all its stages. I would like to thank also Ian Kim for his help with the Chembench system, the members of the Molecular Modeling Lab for providing the datasets, funding, and initiative to make this project possible, each previous Chembench developer, and all of the other students, faculty, and staff of the departments of Computer Science and Chemistry.

References

1. Sedykh, A.; Fourches, D.; Duan, J.; Hucke, O.; Garneau, M.; Zhu, H.; Bonneau, P.; Tropsha, A. Human Intestinal Transporter Database: QSAR Modeling and Virtual Profiling of Drug Uptake, Efflux, and Interactions. *Pharm. Res.* **2013**, *30*, 996-1007.
2. Jones, P. M.; George, A. M. The ABC transporter structure and mechanism: perspectives on recent research. *Cell Mol. Life Sci.* **2004**, *61*(6), 682–99.
3. Hediger, M. A.; Romero, M. F.; Peng, J. B.; Rolfs, A.; Takanaga, H.; Bruford, E. A. The ABCs of solute carriers: physiological, pathological and therapeutic implications of human membrane transport proteins: Introduction. *Pflugers Arch.* **2004**, *447*(5), 465–8.
4. Aller, S. G; Yu, J.; Ward, A.; Weng, Y.; Chittaboina, S.; Zhuo, R.; Harrell, P. M.; Trinh, Y. T.; Zhang, Q.; Urbatsch, I. L.; *et al.* Structure of P-Glycoprotein Reveals a Molecular Basis for Poly-Specific Drug Binding. *Science* **2009**, *323*(5922), 1718-1722.
5. Wikimedia Commons: http://en.wikipedia.org/wiki/File:MDR3_3g5u.png
6. Brown, N. Chemoinformatics--an introduction for computer scientists. *ACM Comput. Surv.* **2009**, *41*(2), 8-38.

7. Brown, F. K. Chapter 35. Cheminformatics: What is it and How does it Impact Drug Discovery. *Ann. Rep. Med. Chem.* **1998**, 33.
8. Russo, E. Chemistry plans a structural overhaul. *Nature Jobs* **2002**, *419*, 4–7.
9. Willett, P. A Bibliometric analysis of chemoinformatics. *Aslib Proc.* **2008**, *60*, 4-17.
10. Hann, M.; Green, R. Chemoinformatics - a new name for an old problem? *Chem. Biol.* **1999**, *3*, 379-383.
11. Chen, W. L. Chemoinformatics: past, present and future. *J. Chem. Inf. Mod.* **2006**, *46*, 2230-2255.
12. Gasteiger, J. Chemoinformatics: a new field with a long tradition. *Anal. Bioanal. Chem.* **2006**, *384*, 57-64.
13. Maldonado, A. G.; *et al.* Molecular similarity and diversity in chemoinformatics: from theory to applications. *Mol. Div.* **2006**, *10*, 39-79.
14. Willett, P. From chemical documentation to chemoinformatics: fifty years of chemical information science. *J. Inf. Sci.* **2008**, *34*, 477-499.
15. Tropsha, A. Best Practices for QSAR model Development, Validation, and Exploitation. *Mol. Inf.* **2010**, *29*, 476-488.
16. Nantasenamat, C.; Isarankura-Na-Ayudhya, C.; Naenna, T.; Prachayasittikul, V. A Practical Overview of Quantitative Structure-Activity Relationship. *EXCLI J.* **2009**, *8*, 74-88.
17. Esposito, E. X.; Hopfinger, A. J.; Madura, J. D.; Methods for Applying the Quantitative Structure-Activity Relationship Paradigm. In *Chemoinformatics: Concepts, Methods, and Tools for Drug Discovery;* Bajorath, J., Ed.; Totowa: New Jersey, **2004**; pp 131-213.
18. OECD Principles for the Validation of (Q)SARs. *European Commission Joint Research Centre*. Institute for Health and Consumer Protection, 30 June **2011**. Web. 19 Apr. 2014.
19. Giacomini, K. M.; Huang, S. M.; Tweedie, D. J.; Benet, L. Z.; Brouwer, K. L. R.; Chu, X.; *et al.* Membrane transporters in drug development. *Nat. Rev. Drug Discov.* **2010**, *9*, 215-36.
20. Saier Jr., M. H.; Yen, M. R.; Noto, K.; Tamang, D. G.; Elkan, C. The transporter classification database: recent advances. *Nucleic Acids. Res.* **2009**, *37*, D274-8.
21. Yee, S. W.; Chen, L.; Giacomini, K. M. Pharmacogenomics of membrane transporters: past, present and future. *Pharmacogenomics* **2010**, *11*, 897-8.

22. Ozawa, N.; Shimizu, T.; Morita, R.; Yokono, Y.; Ochiai, T.; Munesada, K.; *et al.* Transporter database, TP-Search: a web-accessible comprehensive database for research in pharmacokinetics of drugs. *Pharm. Res.* **2004**, *21*, 2133-4.
23. Ren, Q.; Chen, K.; Paulsen, I. T. TransportDB: a comprehensive database resource for cytoplasmic membrane transport systems and outer membrane channels. *Nucleic Acids Res.* **2007**, *35*, D274-9.
24. Gene Database. *National Center for Biotechnology Information.* <http://www.ncbi.nlm.nih.gov/gene/>
25. Golbraikh, A.; Muratov, E.; Fourches, D.; Tropsha, A. Data Set Modelability by QSAR. *J. Chem. Inf. Model.* **2014**, *54*, 1-4.
26. Carolina Cheminformatics Workbench. <chembench.mml.unc.edu>

Appendix

Table 6. Characterization data for continuous datasets.

Transporter	Activity	Hot Ligand [a]	Number of Compounds	Number of Descriptors [b]		Modelability Index [c]	
				CDK	Dragon	CDK	Dragon
Substrate Datasets							
ASBT	pKm		51	127	878	0.234	0.147
MDR1	pKm		63	152	1,015	0.226	0.059
MRP2	pKm		27	148	944	0.081	0.000
PEPT1	pKm		72	133	845	0.411	0.329
Inhibition Datasets							
ASBT	pIC50	Taurocholate	341	159	1,243	0.565	0.576
BCRP	pIC50	Any	119	155	1,096	0.420	0.394
BCRP	pIC50	Mitoxantrone	46	138	902	0.389	0.452
BSEP	pIC50	Taurocholate	295	160	1,215	0.175	0.166
MCT1	pIC50	Any	46	142	955	0.114	0.279
MDR1	pIC50	Any	476	159	1,229	0.378	0.383
MDR1	pIC50	Calcein AM	116	154	1,119	0.374	0.306
MDR1	pIC50	Daunorubicin	302	152	1,164	0.364	0.413
MDR1	pIC50	Vinblastine	48	140	942	0.148	0.167
MRP1	pIC50	Any	196	151	1,056	0.474	0.391
MRP1	pIC50	Calcein AM	54	140	943	0.426	0.236
MRP1	pIC50	Daunorubicin	108	139	951	0.325	0.341
MRP2	pIC50	Any	103	154	1,138	0.344	0.313
MRP2	pIC50	DNP-SG	46	145	971	0.466	0.532
MRP4	pIC50	Any	40	143	987	0.228	0.240
NTCP	pIC50	Taurocholate	75	155	1,099	0.162	0.177
OATP2B1	pIC50	Any	27	146	1,010	0.412	0.202
OCT1	pIC50	Any	87	149	981	0.068	0.207
OCT1	pIC50	Tetraethylammonium	51	148	949	0.196	0.286
PEPT1	pIC50	Any	272	155	1,149	0.412	0.326
PEPT1	pIC50	Glycylsarcosine	269	154	1,147	0.408	0.323

[a] Hot ligands are specified for inhibition datasets. [b] Number of descriptors is the count of informative descriptors retained from an initial 202 CDK and 2489 Dragon descriptors. [c] Modelability indices calculated using equation (2).

Table 7. Characterization data for classification datasets.

Transporter	Activity [a]	Threshold (μM)	Number of Compounds	Number of Descriptors [b]		Modelability Index [c]	
				CDK	Dragon	CDK	Dragon
Substrate Datasets							
ASBT	Substrate		106	144	1,064	0.906	0.877
BCRP	Substrate		169	160	1,227	0.722	0.720
BSEP	Substrate		34	140	924	0.733	0.708
MCT1	Substrate		36	138	835	0.694	0.694
MDR1	Substrate		567	162	1,347	0.686	0.679
MRP1	Substrate		180	160	1,206	0.849	0.817
MRP2	Substrate		222	160	1,192	0.736	0.752
MRP3	Substrate		100	158	1,075	0.870	0.910
MRP4	Substrate		122	159	1,187	0.762	0.713
MRP5	Substrate		58	152	1,092	0.776	0.759
NTCP	Substrate		70	153	1,065	0.786	0.829
OATP2B1	Substrate		59	153	1,046	0.649	0.691
OCT1	Substrate		82	154	1,124	0.866	0.817
PEPT1	Substrate		292	158	1,176	0.807	0.762
Inhibition Datasets							
ASBT	Inhibitor	10	232	159	1,217	0.853	0.780
BCRP	Inhibitor	10	395	162	1,266	0.762	0.762
BSEP	Inhibitor	10	679	162	1,387	0.753	0.740
BSEP	Inhibitor	100	725	162	1,393	0.791	0.763
MCT1	Inhibitor	10	68	147	1,028	0.979	0.954
MDR1	Inhibitor	10	1,585	162	1,420	0.888	0.886
MRP1	Inhibitor	10	426	158	1,242	0.831	0.814
MRP2	Inhibitor	10	104	153	1,127	0.721	0.740
MRP3	Inhibitor	10	36	154	1,048	0.624	0.405
MRP3	Inhibitor	50	35	154	1,061	0.571	0.393
MRP4	Inhibitor	10	67	148	1,069	0.641	0.615
MRP4	Inhibitor	50	69	148	1,074	0.761	0.783
MRP5	Inhibitor	50	37	144	1,030	0.801	0.763
NTCP	Inhibitor	10	127	158	1,171	0.746	0.673
OATP2B1	Inhibitor	100	114	159	1,122	0.737	0.754
OCT1	Inhibitor	100	199	159	1,162	0.779	0.806
PEPT1	Inhibitor	100	82	141	956	0.659	0.610

[a] Substrate datasets distinguish substrates from non-substrates, and inhibitor datasets distinguish inhibitors from non-inhibitors at the given threshold concentration. [b] Number of descriptors is the count of informative descriptors retained from an initial 202 CDK and 2,489 Dragon descriptors. [c] Modelability indices calculated using equation (1).

Table 8. Characterization data for each transporter represented in the database.

Transporter	Gene	Membrane	Direction	Superfamily	Subfamily	Substrate
MDR1	ABCB1	Apical	Efflux	ABC	MDR	Xenobiotics
BSEP	ABCB11	Apical	Efflux	ABC	MDR	Bile Acids
MRP1	ABCC1	Basal	Efflux	ABC	MRP	Organic Anions
MRP2	ABCC2	Apical	Efflux	ABC	MRP	Bile Acids
MRP3	ABCC3	Basal	Efflux	ABC	MRP	Organic Anions
MRP4	ABCC4	Basal	Efflux	ABC	MRP	Cyclic Nucleotides
MRP5	ABCC5	Basal	Efflux	ABC	MRP	Cyclic Nucleotides
BCRP	ABCG2	Apical	Efflux	ABC	White	Xenobiotics
NTCP	SLC10A1	Basal	Influx	SLC	SLC10	Bile Acids
ASBT	SLC10A2	Apical	Influx	SLC	SLC10	Bile Acids
PEPT1	SLC15A1	Apical	Influx	SLC	SLC15	Oligopeptides
MCT1	SLC16A1	Apical	Influx	SLC	SLC16	Monocarboxylates
OCT1	SLC22A1	Basal	Influx	SLC	SLC22	Organic Cations
OATP2B1	SLCO2B1	Apical	Influx	SLC	SLCO	Organic Anions

Table 9. External validation results (R^2, %) for transporter regression predictors.

Trans-porter	Hot Ligand [a]	CDK Descriptors				Dragon Descriptors			
		RF	SVM	GA-kNN [b]	SA-kNN [b,c]	RF	SVM	GA-kNN [b]	SA-kNN [b,c]
Substrate Predictors									
ASBT		27 ± 16	15 ± 39	failed	32 ± 36	27 ± 20	-2 ± 20	14 ± 39	3 ± 29
MDR1		-5 ± 17	12 ± 34	-9 ± 58	22 ± 44	2 ± 30	13 ± 13	6 ± 51	25 ± 28
PEPT1		41 ± 16	23 ± 29	23 ± 24	30 ± 26	23 ± 18	38 ± 17	39 ± 24	45 ± 19
Inhibition Predictors									
ASBT	Tauro.	82 ± 3	80 ± 2	75 ± 9	77 ± 7	79 ± 4	79 ± 3	73 ± 5	81 ± 4
BCRP	Any	53 ± 14	55 ± 8	59 ± 13	51 ± 15	44 ± 7	56 ± 11	60 ± 7	58 ± 8
BCRP	Mitox.	55 ± 25	31 ± 28	failed	failed	36 ± 43	54 ± 18	failed	failed
BSEP	Tauro.	27 ± 10	7 ± 10	failed	---	30 ± 18	37 ± 12	5 ± 18	---
MCT1	Any	21 ± 23	23 ± 35	failed	failed	44 ± 16	33 ± 13	failed	failed
MDR1	Any	55 ± 9	51 ± 10	52 ± 6	---	55 ± 7	57 ± 8	52 ± 7	---
MDR1	Calc.-AM	57 ± 15	50 ± 29	55 ± 6	57 ± 6	60 ± 4	59 ± 10	53 ± 9	56 ± 10
MDR1	Dauno.	57 ± 10	54 ± 11	59 ± 7	---	61 ± 8	60 ± 9	60 ± 6	---
MDR1	Vinbl.	8 ± 55	-12 ± 55	failed	failed	12 ± 34	37 ± 27	failed	failed
MRP1	Any	62 ± 7	64 ± 6	61 ± 9	---	63 ± 5	61 ± 7	59 ± 11	---
MRP1	Calc.-AM	44 ± 24	47 ± 36	27 ± 39	60 ± 20	31 ± 21	45 ± 9	46 ± 29	48 ± 8
MRP1	Dauno.	53 ± 6	54 ± 15	46 ± 11	54 ± 10	49 ± 14	54 ± 5	38 ± 22	50 ± 8
MRP2	Any	29 ± 25	-8 ± 76	42 ± 19	40 ± 11	19 ± 33	55 ± 14	34 ± 8	41 ± 7
MRP2	DNP-SG	50 ± 23	41 ± 35	failed	failed	45 ± 19	68 ± 30	failed	failed
MRP4	Any	11 ± 27	8 ± 17	failed	failed	18 ± 44	12 ± 36	failed	failed
NTCP	Tauro.	27 ± 15	-9 ± 14	9 ± 19	9 ± 11	21 ± 14	-20 ± 62	10 ± 14	10 ± 23
OCT1	Any	34 ± 28	8 ± 41	29 ± 28	34 ± 24	40 ± 20	16 ± 25	33 ± 33	34 ± 30
OCT1	$N(Et)_4$	41 ± 31	34 ± 8	19 ± 45	26 ± 39	27 ± 36	59 ± 15	failed	36 ± 26
PEPT1	Any	46 ± 8	47 ± 16	45 ± 1	---	40 ± 18	39 ± 12	33 ± 19	---
PEPT1	Glycyl.	48 ± 8	27 ± 25	29 ± 21	---	38 ± 13	28 ± 17	33 ± 15	---

Results are mean ± st.dev across five cross-validation folds. All regression predictors were creating using range scaled descriptors. [a] Inhibition datasets are identified by a hot ligand. [b] kNN models of datasets with fewer than 50 compounds failed to pass required cut-offs. [c] kNN-SA models were not created for datasets with more than 150 compounds. No models were created for datasets with fewer than 30 compounds. All successful models were significantly better than y-randomized models (see Methods).

Table 10. External validation results (CCR, %) for classification transporter predictors.

Transporter	Threshold [a] (μM)	CDK Descriptors		Dragon Descriptors	
		Range	Auto	Range	Auto
Substrate Predictors					
ASBT		87 ± 7	88 ± 7	88 ± 9	87 ± 9
BCRP		79 ± 3	75 ± 3	73 ± 4	75 ± 3
BSEP		62 ± 19	68 ± 22	73 ± 18	68 ± 16
MCT1		79 ± 13	76 ± 12	76 ± 12	79 ± 8
MDR1		72 ± 3	72 ± 3	74 ± 5	72 ± 5
MRP1		83 ± 5	85 ± 5	85 ± 7	86 ± 5
MRP2		79 ± 3	79 ± 4	81 ± 5	80 ± 7
PEPT1		86 ± 5	86 ± 5	86 ± 5	86 ± 5
MRP3		89 ± 4	87 ± 7	92 ± 5	91 ± 6
MRP4		75 ± 11	76 ± 9	75 ± 12	75 ± 13
MRP5		76 ± 16	69 ± 18	74 ± 12	76 ± 16
NTCP		89 ± 4	89 ± 6	86 ± 11	83 ± 8
OATP2B1		73 ± 17	71 ± 9	77 ± 13	81 ± 7
OCT1		85 ± 11	87 ± 13	85 ± 6	86 ± 8
Inhibition Predictors					
ASBT	10	88 ± 5	89 ± 5	87 ± 7	87 ± 5
BCRP	10	81 ± 7	79 ± 7	80 ± 5	82 ± 8
MCT1	10	96 ± 5	96 ± 5	93 ± 8	91 ± 7
BSEP	10	83 ± 3	83 ± 3	84 ± 2	84 ± 2
BSEP	100	77 ± 4	77 ± 5	76 ± 3	77 ± 5
MDR1	10	91 ± 2	91 ± 2	91 ± 1	91 ± 2
MRP1	10	84 ± 3	84 ± 4	83 ± 5	83 ± 4
MRP2	10	79 ± 6	78 ± 11	80 ± 7	81 ± 9
MRP3	10	61 ± 15	56 ± 14	60 ± 20	63 ± 16
MRP3	50	48 ± 23	54 ± 15	53 ± 21	57 ± 18
MRP4	10	78 ± 5	73 ± 9	70 ± 11	69 ± 6
MRP4	50	75 ± 17	73 ± 10	76 ± 12	73 ± 11
MRP5	50	73 ± 20	78 ± 18	72 ± 17	70 ± 21
NTCP	10	78 ± 6	79 ± 8	76 ± 9	80 ± 8
OATP2B1	100	79 ± 8	83 ± 7	81 ± 10	80 ± 5
OCT1	100	86 ± 7	86 ± 6	85 ± 7	85 ± 7
PEPT1	100	70 ± 4	74 ± 11	72 ± 6	69 ± 7

Results are mean ± st.dev across five cross-validation folds. All classification predictors were creating using random forests. [a] Inhibition datasets are identified by a threshold concentration. All models were significantly better than y-randomized models (see Methods).